

Robustness of ARS Leptogenesis in Scalar Extensions

Oliver Fischer^{*1}, Manfred Lindner^{†2}, and Susan van der Woude^{‡2}

¹Department of Mathematical Sciences, University of Liverpool, Liverpool, L69 7ZL, UK

²Max-Planck-Institut für Kernphysik, 69117 Heidelberg, Germany

Abstract

Extensions of the Standard Model (SM) with sterile neutrinos are well motivated from the observed oscillations of the light neutrinos and they have shown to successfully explain the Baryon Asymmetry of the Universe (BAU) through, for instance, the so-called ARS leptogenesis. Sterile neutrinos can be added in minimal ways to the SM, but many theories exist where sterile neutrinos are not the only new fields. Such theories often include scalar bosons, which brings about the possibility of further interactions between the sterile neutrinos and the SM. In this paper we consider an extension of the SM with two sterile neutrinos and one scalar singlet particle and investigate the effect that an additional, thermalised, scalar has on the ARS leptogenesis mechanism. We show that in general the created asymmetry is reduced due to additional sterile neutrino production from scalar decays. When sterile neutrinos and scalars are discovered in the laboratory, our results will provide information on the applicability of the ARS leptogenesis mechanism.

1 Introduction

The discovery of the Higgs boson completed the Standard Model (SM) of particle physics [1, 2]. However, there are still some loose ends which the SM is unable to connect. For instance the nature of Dark Matter (DM), the generation of neutrino masses or the observed Baryon Asymmetry of the Universe (BAU) are open questions which call for an extension of the SM. A very efficient theory framework that addresses these three questions simultaneously is the extension of the SM with three right-handed (or sterile) neutrinos. Sterile neutrinos can be introduced explicitly in order to address the observations of neutrino oscillations, BAU, and DM in a minimal way. An excellent example is given by the so-called neutrino minimal Standard Model (ν MSSM) [3, 4, 5], cf. also Ref. [6] for a review.

It was shown by Akhmedov, Rubakov, and Smirnov that the existence of sterile neutrinos can explain the observed BAU via oscillations between the active and the sterile neutrino sectors [7], which is referred to as the ARS leptogenesis mechanism. Within this mechanism CP violating interactions between sterile neutrinos and the active lepton sector result in a lepton number asymmetry in both the sterile and the active neutrino sector. Sphaleron processes will subsequently convert the lepton asymmetry stored in the (left-handed) active sector into a baryon asymmetry [8] thus explaining the Baryon Asymmetry of the Universe. Note that this mechanism, unlike standard thermal leptogenesis [9] or resonant leptogenesis [10], requires the sterile neutrinos to be non-thermal, i.e. the interaction rate with the active leptons must be small. Consequently, ARS leptogenesis requires the sterile neutrinos to have GeV-scale masses. See for example Refs. [11, 12] for recent reviews and Refs. [13, 14] for investigations into the available parameter space of such models.

*oliver.fischer@liverpool.ac.uk

†lindner@mpi-hd.mpg.de

‡susan@mpi-hd.mpg.de

In contrast to adding sterile neutrinos explicitly to the SM, their existence is motivated naturally in non-minimal extensions of the SM, for instance in models where an additional gauge symmetry is introduced. For example, when the $B - L$ numbers of the SM fermions are gauged, a $U(1)_{B-L}$ gauge factor is introduced, together with an additional gauge field and a scalar to make the gauge field massive via spontaneous symmetry breaking. The existence of sterile neutrinos is required in this model to keep the theory anomaly-free [15]. In this case an explicit Majorana mass for the sterile neutrinos would be forbidden, however, it can be introduced dynamically through the same scalar that makes the gauge boson massive. Extensions of the minimal sterile-neutrino framework, and their effect on (ARS) leptogenesis, have been discussed in the context of many different theory frameworks: in conformal models [16, 17]; in $B - L$ extensions [18]; in a Majoron model and axions [19]; in the context of inflatons [20]. Particularly interesting is the observation that resonant leptogenesis can be possible for heavy neutrinos as light as 500 GeV if their decays are assisted by additional scalars [21].

A smoking gun for a non-minimal neutrino sector would be the discovery of additional scalar resonances in the laboratory. Scalar particles are searched for extensively at the LHC and excesses in recent data seem to point toward additional scalar degrees of freedom. The CMS collaboration measured an excess in diphoton events [22] that could be a scalar resonance at about 96 GeV, compatible with an excess in $b\bar{b}$ from LEP, cf. Refs. [23, 24]. Moreover, there are excesses in multi-lepton final states pointing towards a heavy scalar with a mass of about 270 GeV [25, 26] that is connected to diphoton excesses in many signal channels pointing toward a resonance at 151 GeV [27]. Last but not least, there are also some less significant excesses in four-lepton final states with invariant masses around 400 GeV and above [28]. Clearly more data is needed to determine if any of these excesses will turn into a discovery.

In this paper we consider how an additional thermalised scalar would affect the efficiency of the ARS mechanism to address the BAU. Therefore we extend the SM with two right-handed neutrinos and a scalar boson, corresponding to an effective model that can in principle explain both neutrino oscillations and the observed BAU. This model can be interpreted as an extension of the so-called ν MSM [4] or as a $B - L$ symmetric model where the gauge boson is many orders of magnitude heavier than the other SM extending fields.

This article is structured as follows. In Section 2 we will start with a discussion of the model including the sterile neutrinos and the additional scalar. Following this, thermal effects of the scalar on the dynamics of the sterile neutrino will be summarized. Afterwards, the kinetic equations, needed to calculate the lepton asymmetry, will be reviewed and the effect of an additional scalar will be discussed. Section 2 will end with a discussion on the timescales which are relevant for successful leptogenesis via oscillations. Section 3 will start with a general discussion on the available parameter space, where general arguments are used to determine which parameter ranges could lead to non-trivial dynamics. In the remainder of this section results from explicit calculations will be given. The results can be used to determine how the additional scalar affects ARS leptogenesis. The article will be wrapped up with our conclusions.

2 Theory framework

We consider a minimal extension of the scalar sector with a real scalar singlet and a minimal extension of the fermion sector with two right-handed neutrinos (or, analogously, sterile neutrinos). The latter are motivated and constrained by the observed neutrino oscillations and we also consider LHC constraints on scalar resonances for the former, both of these constraints limit the model parameters at zero temperature. As we want to study early Universe cosmological implications of this framework, we also include finite temperature effects.

2.1 The Model

For concreteness we introduce $B - L$ symmetry with a corresponding $U(1)_{B-L}$ gauge factor that is spontaneously broken at an energy scale far above the electroweak scale. In this model the field content

beyond the SM is given by three additional sterile neutrinos N_i , $i = 1, 2, 3$ and a complex scalar singlet S that carries twice the charge of N_i under the $B - L$ symmetry (typically lepton number 2). For the sake of minimality we make two assumptions: the third sterile neutrino N_3 is decoupled and does not contribute to our discussion; the gauge boson corresponding to the $B - L$ symmetry can be neglected, e.g. because its gauge couplings are sufficiently small or its mass is much larger than the other particle's masses. This leaves us with a real scalar boson S and two sterile neutrinos.

In this scenario the following Yukawa terms can be added to the Lagrangian of the SM:

$$\mathcal{L}_Y = -F_{\alpha i} \bar{L}_\alpha H N_i - \frac{1}{2} Y_{ij} S \bar{N}_i^c N_j + (h.c.). \quad (1)$$

Above, H is the SM Higgs field, L_α are the left-handed lepton doublets with $\alpha = e, \mu, \tau$ and N_i with $i = 1, 2$ are the right-handed neutrinos that couple to S with Yukawa-like coupling matrix Y . F is a Yukawa-like coupling matrix describing the interactions between the right-handed neutrinos, the lepton doublet, and the Higgs boson. We work in a basis where the mass matrix of the sterile neutrinos is diagonalized, i.e. the Yukawa matrix Y is a diagonal matrix. We remark at this point that in this model the lightest active neutrino is exactly massless due to the decoupled third sterile neutrino N_3 .

The scalar potential in our model can be expressed as

$$V(S, H) = -\frac{1}{2} \mu_S^2 S^2 - \mu_H^2 H^\dagger H + \frac{1}{4} \lambda_S S^4 + \lambda_H (H^\dagger H)^2 + \frac{1}{2} \lambda_{SH} H^\dagger H S^2, \quad (2)$$

where the μ_i are mass parameters and the λ_i are coupling constants of the scalar fields S and H , where the former is a real scalar field and the latter is the complex isospin doublet of the SM Higgs boson. Notice that terms that are odd in S can be neglected because of the $B - L$ symmetry.

The scalars S and H can develop non-zero vacuum expectation values (vevs) when $\mu_i^2 > 0$:

$$\langle S \rangle = v_S^0, \quad \langle H \rangle = \begin{pmatrix} 0 \\ \frac{1}{\sqrt{2}} v_{EW} \end{pmatrix}, \quad (3)$$

As long as the mixing between the new scalar and the Higgs is small, the physical Higgs is dominated by the neutral component of the doublet H , with $v_{EW} = 246$ GeV. As H has isospin and hypercharge, this leads to spontaneous breaking of the electroweak symmetry as in the SM.

2.2 Parametrisation

The scalar sector contains two independent parameters that will be relevant for our discussion below: the scalar-Higgs coupling λ_{SH} and the scalar self-coupling λ_S . When the scalars S and H develop non-zero vevs, Dirac (M_D) and Majorana (M_M) mass matrices emerge for the neutrinos:

$$M_D = F \cdot v_H, \quad M_M = Y \cdot v_S^0. \quad (4)$$

In the type I seesaw approximation the small neutrino mass is given by M_D^2/M_M . Notice, however, that lepton number is broken in this setup only when the trace of M_M is non-zero. Diagonalisation of the mass matrix yields the physical eigenstates, which are linear combinations of the interaction fields. We anticipate the requirement from leptogenesis for the sterile neutrinos to be quasi degenerate in masses,¹ and introduce the parametrisation:

$$M_\pm = M_N^0 (1 \pm \alpha). \quad (5)$$

¹The leptogenesis mechanism requires the mass splitting between the sterile neutrinos to be small, i.e. the sterile neutrino masses to be highly degenerate. This is true for the ARS mechanism and also for resonant leptogenesis, see refs. [29, 30] for an extended discussion.

m_1	m_2	m_3	$\sin^2 \theta_{12}$	$\sin^2 \theta_{13}$	$\sin^2 \theta_{23}$
0 eV	8.68×10^{-3} eV	5.03×10^{-2} eV	0.307	0.0218	0.545

Table 1: Variables of the ν MSM model, light neutrino observables from the Particle Data Group 2020 [31]

The parameter α parametrises the mass difference of the two heavy neutrinos at zero temperature, and for $\alpha \ll 1$ we have $M_- = |Y_{11}|v_S^0 \simeq |Y_{22}|v_S^0 = M_+$ (in the basis where M_M is diagonal) such that we can approximate the masses for both sterile neutrinos M_{\pm} via the zero-temperature mass

$$M_N^0 = Yv_S^0, \quad (6)$$

where we introduced the new parameter $Y = (|Y_{11}| + |Y_{22}|)/2$ which can be used instead of M_N^0 . This yields the two parameters M_N^0 (or Y) and α , which are independent for $\alpha \ll 1$.

The Yukawa coupling F can be parametrised in a bottom-up and completely general way, based on observable low-energy data, the so-called Casas-Ibarra parametrisation for a $3 + 2$ neutrino sector [32]. For this parametrisation we use the following input parameters: the three neutrino mixing angles θ_{ij} , the three active neutrino masses m_i , the two heavy neutrino mass eigenvalues (parametrised by M_N^0 and α) and the four phases ξ, η, δ and ω . The mixing angles and active neutrino masses are known from neutrino experiments [31], see Table 1.

In order to compare our model to the ARS leptogenesis mechanism in the ν MSM we fix the phases to the values used in Ref. [33]: $\xi = 1, \omega = \pi/4, \delta = 7\pi/4$ and $\eta = \pi/3$. We remark that we checked that random variations of the internal parameters within the 1σ limits of the experimental measurements lead to $\mathcal{O}(1)$ modifications in entries of the Yukawa coupling matrix F .

In summary, in our model there are a total of five parameters that are free within certain limits, namely: $Y, \alpha, v_S^0, \lambda_S$ and λ_{SH} . We will discuss the constraints on these parameters below.

2.3 Constraints

Here we list the considered zero-temperature constraints on the masses of the scalar from the LHC and on the mixing between active and sterile neutrinos. Limits from Early Universe cosmology on the sterile neutrino masses will also be discussed.

Sterile neutrinos: Active-sterile neutrino mixing is constrained from precision measurements of the PMNS matrix, cf. Ref. [34]. Our use of the Casas-Ibarra parametrisation and the considered masses $M_N^0 \leq 100$ GeV renders the resulting mixing parameters small compared to current limits.

For $M_N^0 < 1$ GeV, the decays of N during the recombination period releases entropy into the thermal bath and impacts Big Bang Nucleosynthesis, which in general places strong limits on the mixing and mass parameters and requires in particular $M_N^0 \geq \mathcal{O}(0.1)$ GeV [11].

On the other hand, it has been shown that decaying heavy neutrinos with masses $\mathcal{O}(30)$ MeV [35] and sterile neutrinos that interact with additional scalars can alleviate the Hubble tension [36]. We will limit our discussion to $M_N^0 \geq 0.1$ GeV in the following.

Scalar bosons: Additional scalar degrees of freedom that decay into pairs of gauge bosons have been searched for at the LHC, cf. e.g. the CMS report in Ref. [37]. Non-observation restricts these particles to have masses above a few TeV with current data. On the other hand, the recent LHC data includes excesses in the four-lepton invariant mass spectra that hint at additional resonances around 700 GeV [38, 39]. Even more convincing signals have been reported for some time now in non-resonant multi-lepton channels [40] and recently in diphoton channels with associated production [27], which point at

scalar bosons with masses around the electroweak scale. We therefore conclude that scalars with masses around the TeV scale are well motivated.

The measurement of the SM Higgs boson at 125 GeV limits its possible mixing with other scalar degrees of freedom. For the example of a single additional scalar resonance, this mixing can be constrained via precision measurements of the Higgs boson, and also with direct searches. Current constraints limit the sine of the mixing angle to $\mathcal{O}(0.1)$ [41]. The mixing angle and λ_{SH} are related via

$$\sin \alpha = \lambda_{SH} \frac{v_{EW} v_S^0}{M_S^2 - M_h^2} \quad (7)$$

where $M_h = 125$ GeV is the mass of the observed Higgs boson. If we assume that $M_h \ll M_S \simeq \sqrt{2\lambda_S} v_S^0$, the limit on scalar mixing thus constrains

$$\lambda_{SH} \leq 2 \times 0.1 \lambda_S \frac{v_S^0}{v_{EW}}, \quad (8)$$

which implies that for $v_S^0 > \mathcal{O}(10) \times v_{EW}$ the interaction between the Higgs fields and S can be strong, without affecting experimental constraints on the scalar-Higgs mixing. As we shall see below we will consider $v_S^0 \geq 10^6$, such that this limit can be met even if $\lambda_S \ll 1$.

2.4 Finite Temperature effects

In the early Universe both the scalar S and the Higgs are in the symmetric phase, therefore, if $\mu_i^2 > 0$, none of the particles have explicit mass terms. As discussed above, the scalars S and H can develop non-zero vacuum expectation values, which happens at a specific time in the early Universe, i.e. at $T_{EW} \simeq 140$ GeV for the Higgs boson, corresponding to the electroweak phase transition and sphaleron freezeout. The S symmetry breaking occurs at the temperature T_S . For concreteness, we assume that this temperature is identical to the vev of S , i.e. $T_S = v_S^0$. We implemented the time-dependent vev for S through a numerical approximation of the Heaviside-theta function:

$$v_S(z) = v_S^0 \cdot \frac{1}{e^{-2k(z-T_{EW}/v_S^0)} + 1}, \quad (9)$$

with $k = 10^5$. Furthermore, $z = T_{EW}/T$ is used as ‘‘time’’ variable. We remark that we do not implement a similar time-dependence for v_{EW} as we only consider temperatures above T_{EW} , where $v_{EW} = 0$.

We notice that for $z < 1$ or, equivalently, $T > T_{EW}$, the Higgs field remains in the unbroken phase, there is thus no mixing between the two scalars. Any mixing induced after electroweak symmetry breaking does not affect ARS leptogenesis.

In general particles receive a thermal mass from their interactions with the thermal bath. In particular, the scalar S can be thermalised via its interactions with the Higgs field for λ_{SH} being sufficiently large, its thermal mass at one loop is given by

$$M_S(T)^2 = 2\lambda_S (v_S(T))^2 + \frac{1}{4}\lambda_S T^2 + \frac{1}{6}\lambda_{SH} T^2, \quad (10)$$

with $v_S(T)$ defined through Eq. (9). The first term corresponds to the zero temperature mass $M_S(T=0) = M_S^0$ in the limit where λ_{SH} is negligible. In the following we shall approximate it as follows:

$$M_S^0 = \sqrt{2\lambda_S} v_S^0. \quad (11)$$

This is an excellent approximation for $\lambda_S \gg \frac{v_{EW}}{v_S} \lambda_{SH}$, and we require $v_S \geq 10^6$ GeV and $\lambda_{SH} \geq 10^{-4}$ as discussed below.

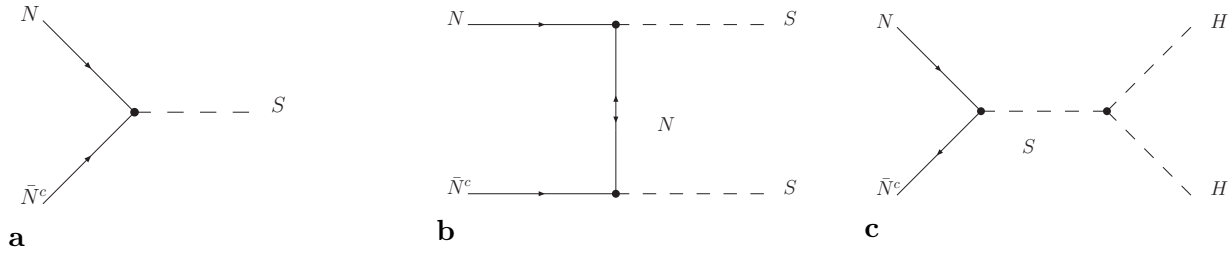


Figure 1: Processes equilibrating N through S .

When the scalar S is in equilibrium with the thermal bath the sterile neutrinos can also obtain a thermal mass from their Yukawa interactions with S [16]:

$$(M_N^2(T))_{ii} = (Y \cdot Y)_{ii} v_S(T)^2 + \frac{2}{3} \frac{1}{8} (Y \cdot Y)_{ii} T^2 \quad (12)$$

for $i = 2, 3$. With $v_s(T)$ defined through Eq. (9). We remark that these thermal masses do not affect the Casas-Ibarra parametrisation, which is defined at zero temperature.

2.5 Leptogenesis

Leptogenesis relies on the existence of processes that fulfil the three Sakharov conditions: they must be out-of-equilibrium, they have to violate CP and they have to violate lepton number. The Sphaleron interactions then translate the lepton asymmetry in the active neutrino sector into a baryon asymmetry. In models with 3 active neutrinos and 2 sterile neutrinos, a lepton asymmetry can be produced via oscillations between the active and the sterile neutrino sectors [33], where the dominant interaction is given by the Higgs boson-mediated process $Nt \rightarrow Lt$, with L the lepton doublets, and t the top quark. The dynamics of the active leptons and right-handed neutrinos are determined via the kinetic equations, which describe the evolution of sterile neutrinos of each helicity ρ_N and $\rho_{\bar{N}}$ as well as the evolution of the SM leptons. For convenience we consider the chemical potential μ_α with lepton flavor $\alpha = e, \mu, \tau$, instead of the number densities for each particle and anti-particle species. The chemical potentials μ_α depend on the specific momentum modes $x = k/T$, which makes solving them rigorously extremely difficult. Fortunately, under the assumption that the sterile neutrino densities are proportional to the equilibrium density, i.e. $\rho_N = R_N \cdot \rho_{eq}$ the kinetic equations can be simplified by taking the thermal average, corresponding to $k = 2T$, without significantly affecting the numerical precision [33]. Note that, like the full kinetic equations, this approximation also conserves the total lepton number, which we explicitly checked. With these approximations the kinetic equations, in terms of $x = k/T$ and $z = T_{EW}/T$, can be written as [33, 42]:

$$\begin{aligned} \frac{dR_N}{dz} \frac{T_{EW}^2}{M_0 z} &= -i[\langle H_N^0 \rangle + \langle V_N \rangle, R_N] - \frac{3}{2} \langle \gamma_N^d \rangle \{F^\dagger \cdot F, R_N - 1\} + 2 \langle \gamma_N^d \rangle F^\dagger \cdot (A - 1) \cdot F \\ &\quad - \frac{\langle \gamma_N^d \rangle}{2} \{F^\dagger \cdot (A^{-1} - 1) \cdot F, R_N\} + \Gamma_S \end{aligned} \quad (13)$$

$$\begin{aligned} \frac{d\mu_\alpha}{dz} \frac{T_{EW}^2}{M_0 z} &= -\gamma_\nu^d(T) [F \cdot F^\dagger]_{\alpha\alpha} \tanh(\mu_\alpha) \\ &\quad + \frac{\gamma_\nu^d(T)}{4} \left(\left(1 + \frac{2}{\cosh(\mu_\alpha)} \right) [F \cdot R_N \cdot F^\dagger - F^* \cdot R_{\bar{N}} \cdot F^T]_{\alpha\alpha} \right. \\ &\quad \left. - \tanh(\mu_\alpha) [F \cdot R_N \cdot F^\dagger - F^* \cdot R_{\bar{N}} \cdot F^T]_{\alpha\alpha} \right) \end{aligned} \quad (14)$$

with $z = T_{EW}/T$, related to time and through the Hubble constant, $H = \frac{1}{2t} = \frac{T^2}{M_0}$, with $M_0 = 7.12 \times 10^{17} \text{GeV}$. The time derivative is thus related to the z derivative as; $\frac{\partial}{\partial t} = \frac{T_{EW}^2}{M_0 z} \frac{\partial}{\partial z}$. Definitions of γ_N^d and

γ_ν^d , coming from the $Nt \rightarrow Lt$ interactions can be found in ref. [33]. Note that $\langle \rangle$ denotes the thermal averaging, for all terms $\sim 1/k$ this corresponds to $k \rightarrow 2T$ in the Maxwell-Boltzmann approximation. By taking the complex conjugate of the kinetic equation of R_N the kinetic equation of $R_{\bar{N}}$ can be obtained straightforwardly.

The kinetic equations used in this paper, like the Boltzmann equations, are valid for relativistic systems close to equilibrium [43]. A full calculation requires the use of so-called Kadanoff-Baym equations, however, it was shown that in the context of thermal leptogenesis the Boltzmann equations are actually able to predict the lepton asymmetry relatively well, see e.g. Ref. [44]. Considering the uncertainty in the predicted BAU due to the other simplifications we have imposed on the kinetic equations, we deem it sufficient to use the kinetic equations as stated above to estimate the BAU.

H_N^0 is the free Hamiltonian $\sqrt{k^2 + (M_N^0)_{ii}^2} \cdot \delta_{ij}$. V_N is the effective potential and contains the medium effects. As mentioned before the tree level mass M_N^0 is defined as

$$(M_N^0)_{ii} = Y_{ii} v_S(z), \quad (15)$$

with $v_S(z)$ defined in Eq. (9). We remark that we are using Maxwell-Boltzmann statistics throughout, unless stated otherwise, thus $\rho_{eq} = e^{-x}$.

V_N is the effective potential of the sterile neutrinos, which describes the interaction with the plasma, is given by

$$V_N = \frac{N_D T^2}{16k} F^\dagger F + \frac{(M_N(T))^2}{2k} = \frac{N_D T^2}{16k} F^\dagger F + \frac{2}{3} \frac{T^2}{16k} Y \cdot Y, \quad (16)$$

with $k = 2T$ in the thermal averaged approximation. Whereas the first term comes from interactions of the sterile neutrino within the SM bath and is included with the ν MSM formalism [33], the second term is due to interactions with the scalar.

The interaction terms in Eq. (1) and Eq. (2) introduce processes that connect the sterile neutrinos with the thermal bath, as shown in Fig. 1. These are the scalar decay (and inverse decay) process **(a)**, t -channel N -scalar boson scattering **(b)**, and s -channel N -Higgs boson scattering **(c)**. We notice that the process **(c)** occurs only after S symmetry breaking and is proportional to the product $(Y\lambda_{SH})^2$ (and is further suppressed by a factor $(T/m_S)^4$ for $T < m_S$), while the process **(b)** is proportional to Y^4 . The decay process **(a)** on the other hand is proportional to Y^2 , which makes it the dominant process for $Y, \lambda_{SH} \ll 1$, such that we neglect the other terms in the following.

We remark that the $U(1)_{B-L}$ gauge boson brings about further interactions between the sterile neutrinos and the SM fermions. If the gauge boson is massless prior to S symmetry breaking N will be in thermal equilibrium at early times. In the following, we shall assume that the gauge boson has interaction rates that are sufficiently suppressed, for instance through a combination of tiny couplings or large gauge boson masses, such that $R_N = 0$ for times that are early compared to the timescale where the ARS leptogenesis mechanism is efficient.

The process **(a)** adds a new term to the kinetic equations, which corresponds to sterile neutrino production from the decays of the scalar S . While S is thermalised with the SM particles, it can act as a source for N and \bar{N} production, via its decay [20, 45]

$$\Gamma_S = \frac{Y \cdot Y}{16\pi} \frac{1}{\rho^{eq}(x)} \frac{M_S(z)^2}{T_{EW}} \frac{z}{x^2} \int_{y_0}^{\infty} n_s(y) dy, \quad (17)$$

with $y_0 = x + \frac{z^2}{4x} \frac{M_s^2}{T_{EW}^2}$ and $n_s(y) = e^{-y}$, i.e. also here the equilibrium density is approximated by the Maxwell-Boltzmann distribution.

We remark here that we consider only production of sterile neutrinos of momentum $k = 2T$, which is fixed through the parameter x in Eq. (17). Sterile neutrino distributions from scalar decay that are not Boltzmann-like should lead to very similar results, since this is the most relevant momentum mode for the ARS mechanism.

The source term in Eq. (17) depends on the coupling parameters, $Y, \lambda_S, \lambda_{SH}$ and v_S^0 through the thermal mass $M_S(T)$ (or $M_S(z)$). Notice that the same process contributes to $\rho_{\bar{N}}$, which is accounted for with a factor 1/2, compared to the decay rate stated in ref. [16]. We remark that this term also acts as a sink for the sterile-neutrino sector through inverse decays, $\bar{N}^c N \rightarrow S$. However, in the following we consider sterile neutrinos to be out of equilibrium, such that inverse decay can be neglected. If the scalar-sterile neutrino interaction would equilibrate long before Sphaleron freeze-out the sterile neutrino sector washout would remove any produced asymmetry.

2.6 Time-scales

It is useful to consider the time scales for understanding the dynamics of leptogenesis [42]. Within ARS leptogenesis there are several important timescales, as we discuss below.

Sphaleron freeze-out: The possibly most important time scale is set by the Sphaleron freeze-out temperature, which happens around $T \sim T_{EW}$. In terms of our time variable z this temperature corresponds to $z = 1$. In order to have efficient Baryon Asymmetry production from the lepton asymmetry in the active sector, lepton asymmetry must be produced *before* Sphaleron freeze-out. Any lepton asymmetry produced after Sphaleron freeze-out is irrelevant for the BAU. The total baryon asymmetry is given by

$$Y_{\Delta B} = -\frac{28}{79}(Y_{\Delta L_e} + Y_{\Delta L_\mu} + Y_{\Delta L_\tau}), \quad (18)$$

where the $Y_{\Delta\alpha}$ correspond to the asymmetries for leptons ℓ_α .

S symmetry breaking: At the temperature T_S the scalar S develops its vev v_S^0 , and as discussed above we assume for simplicity that $T_S = v_S^0$. This implies that at the time $z_S = T_{EW}/T_S = T_{EW}/v_S^0$ the sterile neutrinos and the scalar receive bare masses as defined in Eq. (6) and Eq. (11), respectively. We remark that S can remain thermalised until $z = 1$ as is discussed below.

Oscillations: Another relevant timescale is related to the oscillations within the sterile neutrino sector; t_{osc} . Due to small mass splitting between the two heavy sterile neutrinos each sterile neutrino propagates at a slightly different speed through the plasma; this results in a phase shift between the two sterile neutrinos, which is crucial for developing the lepton asymmetry. This timescale, defined by the time it takes to build up an $\mathcal{O}(1)$ phase difference, can be defined as a function of z as

$$1 = \int_0^{t_{osc}} \frac{\Delta M^2}{4T} dt, \quad (19)$$

where we introduced the sterile neutrino thermal mass splitting:

$$\Delta M^2 = |(M_{N_1}(T))^2 - (M_{N_2}(T))^2|. \quad (20)$$

We notice that the absolute sterile neutrino mass splitting depends on the temperature, such that z_{osc} has to be evaluated via Eq. (19) as a time-dependent quantity.

We remark that for $z \gg z_{osc}$ the oscillations become increasingly fast, and solving the full differential equations becomes computationally expensive. Following [42] we solve the full calculations up to $z = Nz_{osc}$, and for $z_{osc} < z \leq 1$ only the diagonal parts of the differential equation are solved. This is done by setting all off-diagonal components of the right hand side of eq. (14) to zero at $z = z_{osc}$. The factor $N = 20$ is chosen such that Baryon Asymmetry agrees within 0.5% to the full calculations, as was explicitly checked for benchmark point A in Table 2.

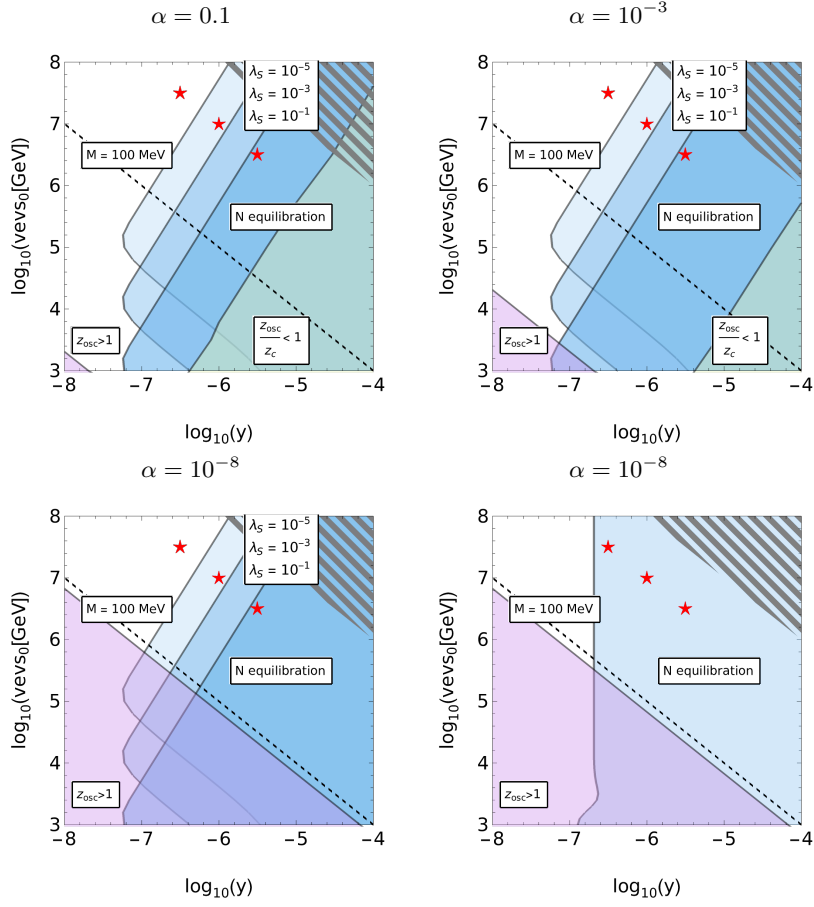


Figure 2: Parameter space with limits from successful leptogenesis as discussed in the text, in the projection Y and y_S . Areas where the process (a) ($S \rightarrow NN$) starts thermalising the sterile neutrinos are shown by the blue color, considering $\lambda_S = 10^{-1}, 10^{-3}, 10^{-5}$. Areas where the active-sterile oscillations occur after Sphaleron freeze-out are shown by the pink color. The green area denotes where $z_S > z_{osc}$. The black hashed corner indicates sterile neutrino masses $M_N \geq 100$ GeV, and the dashed line corresponds to $M_N = 0.1$ GeV. Plotted are the benchmark points A, C and D, cf. Table 2. For the lower right panel, $M_S^0 = 10$ TeV was fixed. Throughout, $\lambda_{SH} = 10^{-3}$ is fixed.

3 Analysis and results

In the following we consider sterile neutrino masses below the electroweak scale, i.e. $M_N^0 \leq 100$ GeV. Such masses are too small to allow for the standard thermal leptogenesis or resonant leptogenesis to produce the observed Baryon Asymmetry. Instead, we will focus on the so-called ARS leptogenesis mechanism, where the asymmetry is produced through oscillations between the active and sterile neutrino sectors.

3.1 Discussion of the parameter space

Among the five model parameters, the limits in Eq. (8) allow for reasonably large mixing, e.g. $\lambda_{SH} \sim \lambda_S$ is allowed for $M_S \geq \mathcal{O}(1)$ TeV and $v_S^0 \geq \mathcal{O}(10)$ TeV. We therefore consider λ_S and λ_{SH} to be free parameters. The other three parameters, α , Y , v_S^0 , are subject to a number of constraints, following the considerations below.

Dominant scalar decay process: We remind ourselves that we assume the dominant N interaction with the thermal bath to be given by process (a), $S \rightarrow \bar{N}N$. This process is only kinematically allowed if the induced thermal mass of the scalar is larger than the thermal mass of the sterile neutrinos, and in

particular Eq. (17) is only correct, if $M_N \ll M_S$. Therefore, our kinematic equations are valid if and only if $\sqrt{\lambda_s} \gg y$. On the other hand, when the process $S \rightarrow N\bar{N}$ is kinematically forbidden one would have to consider the processes (b) and (c) of N -scalar scattering instead, cf. Fig. 1, which is beyond the scope of our discussion.

Out-of-equilibrium N : In Eq. (17) we neglected the inverse decays, which implies that the sterile neutrinos have to have small number densities and thus be out of equilibrium. Explicitly, we chose the condition $\rho_N/\rho_{eq} < 0.15$ at $z = 1$. This choice is conservative: our numerical estimations, for some parameter choices, show that inverse decays are numerically negligible up to $R_N \sim 0.5$. The two considerations above give conditions on both v_S^0 and Y , as functions of λ_S . These constraints are contained in the blue areas in Fig. 2, for different values of λ_S and fixed $\lambda_{SH} = 10^{-3}$.

Early oscillations: As discussed above, active-sterile oscillations need to happen before Sphaleron freeze-out, such that the phase difference between the sterile neutrinos can create a Lepton asymmetry in the active sector that can be translated into a baryon asymmetry. Since Sphalerons freeze-out at $z = 1$ the oscillations need to produce an order one phase shift before this time, which requires for the oscillation time: $z_{osc} < 1$. For different values of the mass splitting α this condition constrains on Y and v_S^0 through the definition of the thermal mass in Eq. (12). The regions where oscillations are too slow are denoted by the pink areas in Fig. 2.

Relativistic N : Sterile neutrinos must remain relativistic up to $z = 1$, such that the two helicity states of the sterile neutrino remain distinct. Moreover, N being relativistic also suppresses the amount of decays $N \rightarrow LH$, compared to the $2 \rightarrow 2$ interaction, thus validating neglecting this decay throughout. These considerations limit the sterile neutrino masses to $m_N \leq T_{EW}$. This implies that the black hashed area in Fig. 2 is nonphysical.

Thermalised scalar: Our kinetic equations, as well as the decay rate into sterile neutrinos, make the implicit assumption that S is in thermal equilibrium with the thermal bath for $v_S \geq T \geq T_{EW}$. For these temperatures the dominant interactions between S and the SM is given by the $SSH^\dagger H$ term in Eq. (2). We compute the interaction rate for the process $H^\dagger H \leftrightarrow SS$ as:

$$\Gamma = \sigma n(T), \quad (21)$$

where $n \propto T^3$ is the density of scalar bosons in the thermal plasma and $\sigma \propto \lambda_{SH}^2/T^2$ is the thermal cross section for this process. We evaluate the thermal cross section with the simplifying assumptions of massless Higgs bosons, and all external scalars having energies $E = 2T$. With this, and neglecting the finite mass M_S ,² the reaction rate is identical to the Hubble rate under the condition

$$\lambda_{SH} > 2.4 \cdot 10^{-7} \sqrt{\frac{T}{\text{GeV}}}. \quad (22)$$

Since we know that relevant dynamics require T not to be too much larger than T_{osc} , let us consider $T \leq 10^4 \cdot T_{EW}$. The assumption that S is thermalised for $z \geq 10^{-4}$ thus yields the condition: $\lambda_{SH} \geq 3 \cdot 10^{-4}$. In the following we shall always consider values for λ_{SH} , such that the condition in Eq. (22) is met.

Time of scalar symmetry breaking: We have to consider the ordering of the two times z_S and z_{osc} . The parameter choice $z_S > z_{osc}$ indicates that S symmetry breaking occurs relatively late, and that the sterile neutrino dynamics are dominated by their thermal mass rather than a fixed mass as is the case in the ν MSM. This area is shown by the green areas in the upper panels of Fig. 2. The parameter choice $z_S < z_{osc}$ is expected to be dynamically closer to the ν MSM.

²The interaction rate drops quickly for $T \leq M_S$ due to phase space suppression. This is accounted for in the definition of the S decay rate into sterile neutrinos Eq. (17).

Points	α	$\langle S \rangle [\text{GeV}]$	y	λ_S	$Y_{\Delta B}$	remarks
A	10^{-8}	$10^{7.5}$	$10^{-6.5}$	10^{-2}	5.04×10^{-11}	equivalent to νMSM
B	10^{-1}	$10^{3.5}$	10^{-6}	10^{-5}	~ 0	Within yellow area
C	10^{-8}	10^7	10^{-6}	10^{-2}	4.96×10^{-11}	relevant production of N
D	10^{-8}	$10^{6.5}$	$10^{-5.5}$	10^{-2}	1.46×10^{-11}	large production of N
E	10^{-8}	10^8	$10^{-6.5}$	10^{-9}	2.5×10^{-10}	“enhancement”

Table 2: Considered parameter space points A, B, C and D . The parameters are the relative mass splitting α , the sterile neutrino Yukawa coupling Y , the zero-temperature vev of the scalar singlet v_S^0 , the scalar singlet self coupling λ_S . Given are the produced Baryon Asymmetry of the Universe $Y_{\Delta B}$ for each point, where the scalar-Higgs coupling $\lambda_{SH} = 10^{-3}$ has been fixed.

3.2 Successful leptogenesis

It is important to realise that the process **(a)**, cf. Eq. (17), creates sterile neutrinos and sterile anti-neutrinos in equal numbers and therefore by itself does not produce any asymmetry in the sterile sector. However, this process acts as a source for sterile neutrinos and thus increases R_N and $R_{\bar{N}}$, which affects the lepton asymmetry production in the active sector via the kinetic equations. For the discussion below we define a number of benchmark parameter points, listed in tab. 2, that correspond to different parameter space regions where successful leptogenesis is possible in principle.

A: The limit of the νMSM : First, we consider the kinetic equations in Eq. (14) only, and use a fixed mass for the sterile neutrinos $M_N^0 = 10 \text{ GeV}$, $\alpha = 10^{-8}$, which corresponds to the case considered in Ref. [33]. Solving the kinetic equations the total baryon asymmetry with the initial conditions $R_N = 0$, $R_{\bar{N}} = 0$, $\mu_\alpha = 0$, $R_N(z)$, $R_{\bar{N}}(z)$ and $\mu_\alpha(z)$, we find the value $Y_{\Delta B} = -\frac{28}{79}Y_{\Delta L_{tot}} = 5.05 \times 10^{-11}$. This value differs by a factor of about four from the results in [33], namely $Y_B = 2.73 \times 10^{-10}$, which we checked is due to the different set of neutrino parameters.

Next we consider the benchmark point A, as defined in Table 2, with the choice of $T_S \gg T_{EW}$. The small Yukawa coupling Y makes the thermal contributions to the sterile neutrino mass negligible for $z \sim z_{osc}$, compared to its vev-induced mass of 10 GeV. This benchmark point corresponds to the limiting case where the scalar interactions are negligible, and indeed the resulting asymmetry is identical to the one evaluated above.

B: Late S symmetry breaking: The case where the scalar S develops its vev after the onset of neutrino oscillations defines $z_S > z_{osc}$. This, combined with the above discussed conditions show that only benchmark points with large relative mass splitting, small v_S^0 , and relatively large Yukawa couplings can at least in principle generate an asymmetry, cf. the left panel of Fig. 2. These parameters result in small sterile neutrino masses after the electroweak symmetry breaking, which in turn suppresses the magnitude of the Yukawa matrix F . As analytic estimates from Ref. [7] make us expect, the resulting baryon asymmetry from benchmark point B is consistent with zero, within computational uncertainties, cf. Table 2.

C, D: Early S symmetry breaking: Early breaking of the symmetry related to S implies $z_S < z_{osc}$. In this regime the sterile neutrino mass is generally dominated by the zero temperature mass, i.e. it is temperature independent in very good approximation, and the oscillations are controlled by $M_N^0 = Y v_S^0$ for $T < v_S^0$. The dynamics are very similar to that of the νMSM , except for the additional N production via the process **(a)**. The boundary of the blue area in the four panels of Fig. 2 indicates where N

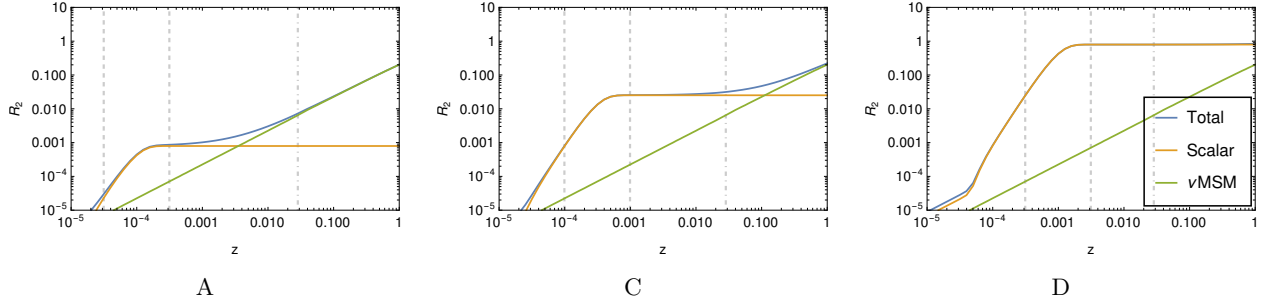


Figure 3: Production of the sterile neutrino density R_N as a function of the time parameter z for the benchmark points A, C, D. The orange and blue line denotes total N production and N production via process **a**, respectively. The green line denotes sterile neutrino production from ν MSM dynamics. The vertical dashed lines indicate the time where S decays are relevant, the dashed-dotted lines correspond to $z = z_{osc} = 0.028$.

production from S decays increases the abundance of sterile neutrinos in the thermal bath to the point, where inverse decays become relevant. Parameter space points that are in the white area and close to the boundary with the blue area are expected to have enhanced production of sterile neutrinos.

The benchmark point C with $M_N^0 = 10$ GeV is close to this boundary for $\lambda_S = 10^{-3}$ and we notice that the resulting asymmetry is slightly reduced, compared to the result from benchmark point A. For comparison we also show the benchmark point D, which is inside the blue area and has a further reduced asymmetry compared to C. Notice that, strictly speaking, the point D violates our assumption that the sterile neutrino densities are negligible. Estimates for the predicted BAU when inverse decay is included show that for moderate sterile neutrino production the suppression of lepton asymmetry production is actually reduced. This is a consequence of the reduced sterile neutrino abundance due to the inclusion of inverse decays. However, to fully understand the dynamics in the blue region more precise calculations are required, ideally including the momentum dependence or for example including more production channels, which is beyond the scope of this work.

3.3 The effect of enhanced N production

We noticed above that leptogenesis can be successful only in the white regions of the parameter space, and that quantitative differences to the ν MSM are to be expected only when N production is not negligible, on the other hand, we expect that too large N production will suppress the asymmetry production. Therefore we inspect the parameter space points that are at the boundary between the white and the blue area in Fig. 2 more closely.

Evolution of R_N : The evolution of the sterile neutrino density R_N with z for the benchmark points A, C and D, is shown in Fig. 3, wherein the blue line denotes production only via S decays while the orange line includes the complete kinetic equations. (Notice that the evolution of $R_{\bar{N}}$ is almost identical, apart from phase differences and from the relatively tiny difference that makes the asymmetry parameters.) The figure shows that for the benchmark points A and C the sterile neutrino density R_N remains below the equilibration limit of 0.15 at $z = 1$. The point D, however, reaches equilibration for $z \simeq 10^{-3}$, which renders its result unphysical as the inverse decays have been neglected. We observe that the main production of sterile neutrinos through scalar decay occurs for $T \sim \mathcal{O}(0.1)M_s(z)$, this region is denoted by the dashed grey lines in plots. For comparison the oscillation timescale is also shown in the plots as the dash-dotted lines.

Varying the scalar vev: As discussed above, in the limit of large vev and early S symmetry breaking, we reproduce the results of the ν MSM. Considering the effect of increased N production, we keep the

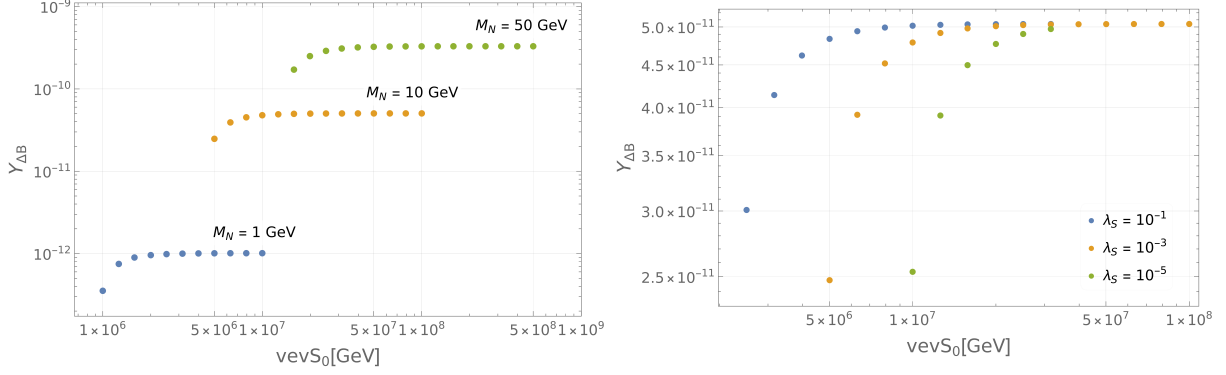


Figure 4: Baryon asymmetry production as a function of the S vacuum expectation value v_S^0 . *Left:* The three lines correspond to fixed sterile neutrino masses $M_N^0 = 1, 10, 50$ GeV. The S self coupling has been fixed to $\lambda_S = 10^{-3}$. *Right:* The three lines correspond to S self couplings $\lambda_S = 10^{-5}, 10^{-3}, 10^{-1}$. The sterile-neutrino mass has been fixed to $M_N^0 = 10$ GeV. For this figure $\lambda_{SH} = 10^{-3}$ has been fixed.

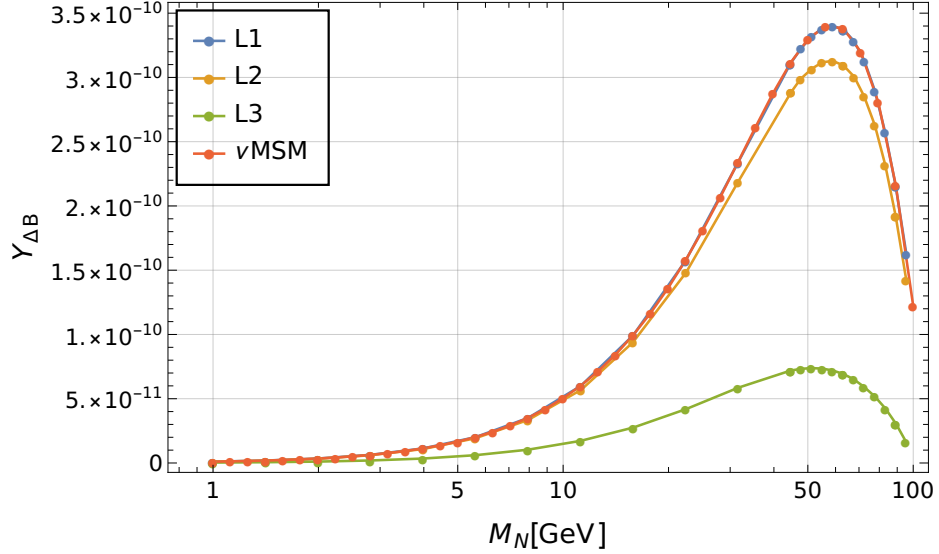


Figure 5: Total baryon asymmetry production as a function of the sterile neutrino mass M_N^0 . The three lines L_1, L_2, L_3 are chosen parallel to the blue area. The remaining parameters are fixed to $\lambda_{SH} = 10^{-3}$, $\lambda_S = 10^{-2}$ and $\alpha = 10^{-8}$. See text for more details.

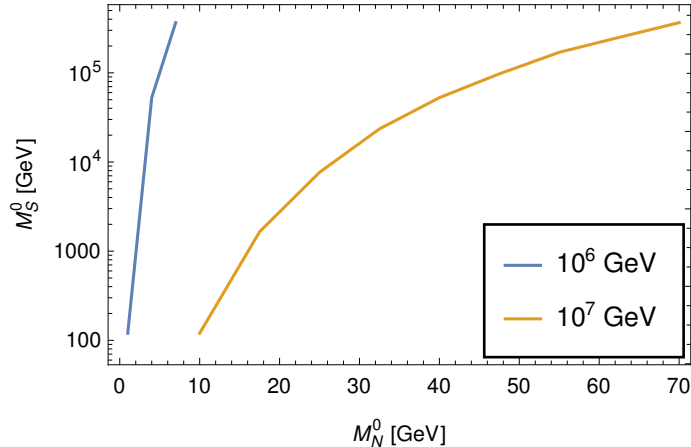


Figure 6: Scalar zero-temperature mass versus sterile neutrino zero-temperature mass. Under the assumption of a value for v_S^0 , successful leptogenesis limits the two masses above the corresponding colored line.

zero temperature neutrino mass M_N^0 fixed and vary v_S^0 , which implies that Y co-varies with the vev as M_N^0/v_S^0 .

The left panel of Fig. 4 shows three lines for fixed $M_N = 1, 10, 50$ GeV, for each M_N the self-coupling $\lambda_S = 10^{-3}$ is fixed. The right panel shows three lines for fixed $\lambda_S = 10^{-5}, 10^{-3}, 10^{-1}$, and $M_N^0 = 10$ GeV is fixed. In both panels $\lambda_{SH} = 10^{-3}$ is used. Both panels show that the asymmetry is reduced for smaller v_S^0 .

The figure shows clearly how the asymmetry converges towards a fixed value when the interaction rate drops below some critical threshold. Conversely the asymmetry drops with decreasing v_S^0 due to increased washout from additional sterile neutrino production through S decays for increasing Y . The onset of the asymmetry reduction depends on the value of Y , as shown in the left panel, as well as the scalar mass M_S , as shown in the right panel.

Varying the sterile neutrino mass: Here we consider the effect of varying sterile neutrino mass on the total baryon asymmetry production for different benchmark points. Therefore we consider pairs of parameters (v_S^0, Y) that are on a line parallel to the blue boundary in Fig. 2. We parametrise this line as

$$\log(v_S^0) = 2 \log(Y) + L_i, \quad (23)$$

where we fix $L_i = 20, 18.5, 17.5$, which is, respectively, far away, close to, and inside the blue area for $\lambda_S = 10^{-2}$. We pick parameter points on these lines for $1 \text{ GeV} \leq M_N^0 \leq 100 \text{ GeV}$, and we fix $\lambda_{SH} = 10^{-3}$ and $\alpha = 10^{-8}$ for definiteness.

The resulting baryon asymmetry for each mass is shown in Fig. 5, where the lines L_1, L_2, L_3 are denoted by the blue, orange, and green line, respectively, and where we show the result for the ν MSM with the red line for comparison. The figure shows clearly how the distance from the blue boundary determines the amount of washout and thus reduces the asymmetry production.

The enhancement for $M_N^0 \sim 60$ GeV can be explained as follows: increasing M_N^0 also increases the Yukawa coupling between the sterile and active sector (through Casas-Ibarra parametrization), which increases the oscillation speed and therefore the asymmetry production. However, at some point the Yukawa coupling becomes so large that sterile neutrinos start to thermalise with the SM bath, and the resulting washout again reduces the produced asymmetry.

3.4 Discussion

Implications of successful leptogenesis: We have seen that the dominant effect of additional scalars, in the parameter ranges discussed, is increased washout, such that successful leptogenesis imposes strong

constraints on the possible values of Yukawa couplings Y , scalar self couplings λ_S , and the vev v_S^0 . Parameters that do not interfere with the leptogenesis mechanism are tiny Yukawa couplings with $Y \leq \mathcal{O}(10^{-7})$ and/or large vevs with $v_S^0 \geq \mathcal{O}(10^8)$ GeV, which corresponds to the decoupling limit. Conversely, combinations of parameters where Y and v_S^0 are both very small lead to very small M_N^0 and thus to oscillations that are too slow to generate an appreciable asymmetry before Sphaleron freeze out.

The domain with moderate vevs below the decoupling limit 10^6 GeV $\leq v_S^0 \leq 10^8$ GeV and Yukawa couplings $Y \geq 10^{-7}$ warrants further scrutiny. In general also in this domain the generated asymmetry is reduced compared to the decoupling limit. For a fixed value of v_S^0 we can define the limiting value for λ_S (or equivalently M_S^0)³ where the generated asymmetry is half that of the asymmetry in the decoupling limit. This allows us to define a minimum scalar mass for each sterile neutrino mass, for which leptogenesis is successful. The resulting limits are shown in Fig. 6, where the colored lines correspond to different values for v_S^0 .

This figure can be interpreted as follows. If scalar particles and sterile neutrinos are discovered, and their masses are below one of the colored lines, the corresponding vev has to be larger, or leptogenesis is not successful. As an example, consider $M_S^0 = 270$ GeV as motivated by the LHC multi-lepton anomalies [25, 26]. Our findings imply that the corresponding M_N^0 has to be smaller than 1 GeV or 12 GeV if $v_S^0 = 10^6$ or $v_S^0 = 10^7$, respectively. If N with larger masses are discovered, this implies $v_S^0 \geq 10^8$ GeV, or that the BAU has to be generated in another way.

Generalisation to multiple scalars: Here we considered the extension of the SM with sterile neutrinos and a single scalar field. In scenarios where the SM is extended with sterile neutrinos and n scalar singlet fields the sterile neutrinos can be even more connected to the thermal plasma, the zero-temperature masses of the sterile neutrinos and the sterile neutrino source terms are given by, respectively,

$$M_N^0 = \sum_i Y_i v_{S_i}^0, \quad \Gamma_{S_i} = \frac{Y_i \cdot Y_i}{16\pi} \frac{1}{\rho^{eq}(x)} \frac{M_{S_i}(z)^2}{T_{EW}} \frac{z}{x^2} \int_{y_{0_i}}^{\infty} n_s(y) dy, \quad (24)$$

where Y_i and v_{S_i} are the Yukawa coupling and vev of the scalar S_i . The Γ_{S_i} are relevant for our discussion if and only if S_i is thermalised and its mass $M_{S_i}^0$ is comparable to the oscillation time, T_{EW}/z_{osc} .

This brings the additional degree of freedom to increase the zero-temperature mass of the sterile neutrinos without increasing the washout, if a dominant contribution stems from a non-thermalised or very heavy scalar. This is comparable to allowing for Majorana mass terms. In general we expect that in these scenarios the resulting asymmetry will be reduced by additional washout.

Enhanced asymmetry production: A limited enhancement of the produced BAU is found for extremely small values of λ_S , relatively small values of Y and large values of v_S^0 , i.e. inside the blue area in fig. Fig. 2. The enhancement seems to occur when the timescales of scalar decays and sterile neutrino oscillations coincide. As an explicit example we discuss benchmark point E, see Table 2, for this point the BAU is enhanced by about 10% compared to the decoupling limit; from respectively 2.34×10^{-10} in the decoupling limit to 2.5×10^{-10} for benchmark point E. This enhancement occurs for rather large R_N production ($R_{N_2} \sim \mathcal{O}(1)$ at $z = 1$). Thus, for a proper calculation of the BAU, inverse decay processes should be taken into account. As discussed before, this will reduce the predicted enhancement, according to our estimates the enhancement is in fact almost completely removed. We consider it unlikely that the enhancement will increase significantly in a full treatment when for example other momentum modes or inverse decays are taken into account properly.

Furthermore, we noticed that the sterile neutrino thermal mass (cf. Eq. (12)) increases the oscillations in the sterile sector, which in turn enhances the asymmetry production in the active one. However, in

³We remark that the mass M_S^0 is obtained from diagonalising the scalar mass matrix, which includes an off-diagonal entry proportional to $\lambda_{SH} v_S^0 v_{EW}$. The condition that S is thermalised, $\lambda_{SH} \geq \mathcal{O}(10^{-4})$ then gives a lower limit for M_S^0 for $\lambda_S < v_{EW}/v_S^0 \lambda_{SH}$.

regions of parameter space where this effect is relevant, it is overcompensated by the enhanced washout from scalar decays. If these two effects could be separated, a significant enhancement of the asymmetry production would be possible. One way of separating these two effects is to have the time of S symmetry breaking after the onset of oscillations, $z_S > z_{osc}$. Parameters that realise this are denoted by the green area in Fig. 2. However, they all lead to thermalisation of N .

In general, the asymmetry production is enhanced when the sterile neutrinos are more degenerate in mass. However, the asymmetry production can also be enhanced without strong mass degeneracy when three flavors of sterile neutrinos are considered, as discussed in e.g. Ref. [46].

Another way that allows to separate zero-temperature sterile neutrino mass, finite temperature sterile neutrino oscillations, and the scalar decay into sterile neutrinos is given by a combination of thermalised and non-thermalised scalars, as discussed above. However, this goes beyond the scope of this work.

Time of scalar symmetry breaking: For our numerical evaluation we have set the time scale T_S at which the S symmetry breaks and $v_S(T) \simeq v_S^0$ equal to the vev itself: $T_S = v_S^0$. The time of symmetry breaking can be evaluated analytically if the field content of the theory is fixed, as is done for the case of the SM, for instance in Ref. [47]. From these arguments we expect that the time of symmetry breaking is proportional to

$$T_S \propto \frac{v_S^0}{\sqrt{\lambda_S}} \quad (25)$$

while the proportionality factors involve ratios of masses of possible additional field content. It is worth pointing out that, in the case of the SM, the energy scale of the symmetry breaking time $1/T_{EW} < v_{EW}$. For our numerical evaluations we find that the exact time of symmetry breaking is irrelevant, as long as it occurs before the relevant time scales of leptogenesis. In particular, symmetry breaking has to occur before the oscillations, which take place typically at $T_{osc} = \mathcal{O}(0.01)T_{EW}$. Therefore the corresponding energy scale of $T_S > 10^4$ GeV is sufficient not to introduce numerical effects on the asymmetry calculation.

4 Conclusions

Sterile neutrinos are well motivated from the light neutrino oscillations and they have been shown to successfully explain the Baryon Asymmetry of the Universe (BAU) through so-called ARS leptogenesis. Sterile neutrinos can be added in theories that include also other new fields, such as scalar bosons, which brings about the possibility of further interactions between the sterile neutrinos and the SM.

In this paper we considered an extension of the SM with two sterile neutrinos and one scalar singlet field in order to study the robustness of the ARS leptogenesis mechanism with respect to scalar extensions. We took into account constraints from the light neutrino parameters and also discussed limits on the scalar sector from LHC searches. We investigated the effect that the thermalised scalar has on the ARS leptogenesis mechanism.

We found that in our model the BAU of the ν MSM is reproduced when the vev is at least as large as $\mathcal{O}(10^8)$ GeV and the Yukawa and scalar self couplings are at most of $\mathcal{O}(10^{-6})$, which we refer to as the decoupling limit. In most of the remaining parameter space the thermalised scalar leads to enhanced sterile neutrino production at early times, resulting in a reduction of the predicted BAU compared to the decoupling limit. A small enhancement of the BAU of $\mathcal{O}(10\%)$ is present for parameters close to the decoupling limit, i.e. $v_S^0 \sim 10^8$ GeV and for scalar and heavy neutrino masses around and below the weak scale, respectively.

Our results are general for models with scalar singlets and with extended gauge sectors, provided that the additional field content does not thermalise the sterile neutrinos at any point of the Universe's history. They can also be generalised to models with more than one scalar field, in which case the sterile neutrino zero-temperature mass and the scalar decay rate are sums over the scalar field content. In such models the zero-temperature sterile neutrino mass could be dominated by a scalar that is not thermalised, such

that the Yukawa couplings in the sterile neutrino masses can be different from those in the decay rate of the thermalised scalar.

Our results can be useful when sterile neutrinos and scalar particles are discovered in the laboratory, such that their masses and the Yukawa coupling are known. In this case it is possible to infer whether or not the ARS mechanism is a valid possibility to create the BAU, or if another mechanism has to be invoked.

References

- [1] Georges Aad et al. Observation of a new particle in the search for the Standard Model Higgs boson with the ATLAS detector at the LHC. *Phys. Lett. B*, 716:1–29, 2012.
- [2] Serguei Chatrchyan et al. Observation of a New Boson at a Mass of 125 GeV with the CMS Experiment at the LHC. *Phys. Lett. B*, 716:30–61, 2012.
- [3] Takehiko Asaka and Mikhail Shaposhnikov. The ν MSM, dark matter and baryon asymmetry of the universe. *Phys. Lett. B*, 620:17–26, 2005.
- [4] Takehiko Asaka, Steve Blanchet, and Mikhail Shaposhnikov. The nuMSM, dark matter and neutrino masses. *Phys. Lett. B*, 631:151–156, 2005.
- [5] Mikhail Shaposhnikov. The nuMSM, leptonic asymmetries, and properties of singlet fermions. *JHEP*, 08:008, 2008.
- [6] K. N. Abazajian et al. Light Sterile Neutrinos: A White Paper. 4 2012.
- [7] Evgeny K. Akhmedov, V. A. Rubakov, and A. Yu. Smirnov. Baryogenesis via neutrino oscillations. *Phys. Rev. Lett.*, 81:1359–1362, 1998.
- [8] Frans R. Klinkhamer and N. S. Manton. A Saddle Point Solution in the Weinberg-Salam Theory. *Phys. Rev. D*, 30:2212, 1984.
- [9] M. Fukugita and T. Yanagida. Baryogenesis Without Grand Unification. *Phys. Lett. B*, 174:45–47, 1986.
- [10] Apostolos Pilaftsis and Thomas E. J. Underwood. Resonant leptogenesis. *Nucl. Phys. B*, 692:303–345, 2004.
- [11] Laurent Canetti, Marco Drewes, Tibor Frossard, and Mikhail Shaposhnikov. Dark Matter, Baryogenesis and Neutrino Oscillations from Right Handed Neutrinos. *Phys. Rev. D*, 87:093006, 2013.
- [12] M. Drewes, B. Garbrecht, P. Hernandez, M. Kekic, J. Lopez-Pavon, J. Racker, N. Rius, J. Salvado, and D. Teresi. ARS Leptogenesis. *Int. J. Mod. Phys. A*, 33(05n06):1842002, 2018.
- [13] Laurent Canetti and Mikhail Shaposhnikov. Baryon Asymmetry of the Universe in the NuMSM. *JCAP*, 09:001, 2010.
- [14] S. Eijima, M. Shaposhnikov, and I. Timiryasov. Parameter space of baryogenesis in the ν MSM. *JHEP*, 07:077, 2019.
- [15] J. C. Montero and V. Pleitez. Gauging U(1) symmetries and the number of right-handed neutrinos. *Phys. Lett. B*, 675:64–68, 2009.
- [16] Valentin V. Khoze and Gunnar Ro. Leptogenesis and Neutrino Oscillations in the Classically Conformal Standard Model with the Higgs Portal. *JHEP*, 10:075, 2013.

- [17] Valentin V. Khoze and Alexis D. Plascencia. Dark Matter and Leptogenesis Linked by Classical Scale Invariance. *JHEP*, 11:025, 2016.
- [18] Andrea Caputo, Pilar Hernandez, and Nuria Rius. Leptogenesis from oscillations and dark matter. *Eur. Phys. J. C*, 79(7):574, 2019.
- [19] Miguel Escudero and Samuel J. Witte. The hubble tension as a hint of leptogenesis and neutrino mass generation. *Eur. Phys. J. C*, 81(6):515, 2021.
- [20] Mikhail Shaposhnikov and Igor Tkachev. The nuMSM, inflation, and dark matter. *Phys. Lett. B*, 639:414–417, 2006.
- [21] Tommi Alanne, Thomas Hugle, Moritz Platscher, and Kai Schmitz. Low-scale leptogenesis assisted by a real scalar singlet. *JCAP*, 03:037, 2019.
- [22] Albert M Sirunyan et al. Search for a standard model-like Higgs boson in the mass range between 70 and 110 GeV in the diphoton final state in proton-proton collisions at $\sqrt{s} = 8$ and 13 TeV. *Phys. Lett. B*, 793:320–347, 2019.
- [23] Junjie Cao, Xiaofei Guo, Yangle He, Peiwen Wu, and Yang Zhang. Diphoton signal of the light Higgs boson in natural NMSSM. *Phys. Rev. D*, 95(11):116001, 2017.
- [24] T. Biekötter, M. Chakraborti, and S. Heinemeyer. A 96 GeV Higgs boson in the N2HDM. *Eur. Phys. J. C*, 80(1):2, 2020.
- [25] Stefan von Buddenbrock, Nabarun Chakrabarty, Alan S. Cornell, Deepak Kar, Mukesh Kumar, Tanumoy Mandal, Bruce Mellado, Biswarup Mukhopadhyaya, Robert G. Reed, and Xifeng Ruan. Phenomenological signatures of additional scalar bosons at the LHC. *Eur. Phys. J. C*, 76(10):580, 2016.
- [26] Stefan von Buddenbrock, Alan S. Cornell, Abdualazem Fadol, Mukesh Kumar, Bruce Mellado, and Xifeng Ruan. Multi-lepton signatures of additional scalar bosons beyond the Standard Model at the LHC. *J. Phys. G*, 45(11):115003, 2018.
- [27] Andreas Crivellin, Yaquan Fang, Oliver Fischer, Abhaya Kumar, Mukesh Kumar, Elias Malwa, Bruce Mellado, Ntsoko Rapheeha, Xifeng Ruan, and Qiyu Sha. Accumulating Evidence for the Associate Production of a Neutral Scalar with Mass around 151 GeV. 9 2021.
- [28] Georges Aad et al. Search for heavy Higgs bosons decaying into two tau leptons with the ATLAS detector using pp collisions at $\sqrt{s} = 13$ TeV. *Phys. Rev. Lett.*, 125(5):051801, 2020.
- [29] Juraj Klarić, Mikhail Shaposhnikov, and Inar Timiryasov. Uniting Low-Scale Leptogenesis Mechanisms. *Phys. Rev. Lett.*, 127(11):111802, 2021.
- [30] Juraj Klarić, Mikhail Shaposhnikov, and Inar Timiryasov. Reconciling resonant leptogenesis and baryogenesis via neutrino oscillations. *Phys. Rev. D*, 104(5):055010, 2021.
- [31] P. A. Zyla et al. Review of Particle Physics. *PTEP*, 2020(8):083C01, 2020.
- [32] J. A. Casas and A. Ibarra. Oscillating neutrinos and $\mu \rightarrow e, \gamma$. *Nucl. Phys. B*, 618:171–204, 2001.
- [33] Takehiko Asaka, Shintaro Eijima, and Hiroyuki Ishida. Kinetic Equations for Baryogenesis via Sterile Neutrino Oscillation. *JCAP*, 02:021, 2012.
- [34] Stefan Antusch and Oliver Fischer. Non-unitarity of the leptonic mixing matrix: Present bounds and future sensitivities. *JHEP*, 10:094, 2014.

- [35] Graciela B. Gelmini, Alexander Kusenko, and Volodymyr Takhistov. Possible Hints of Sterile Neutrinos in Recent Measurements of the Hubble Parameter. *JCAP*, 06:002, 2021.
- [36] Enrique Fernandez-Martinez, Mathias Pierre, E. Pinsard, and Salvador Rosauero-Alcaraz. Inverse Seesaw, dark matter and the Hubble tension. 6 2021.
- [37] Dennis Roy. Searches for heavy resonances decaying into Z, W and Higgs bosons at CMS. *PoS, ICHEP2020*:275, 2021.
- [38] Paolo Cea. Evidence of the true Higgs boson H_T at the LHC Run 2. *Mod. Phys. Lett. A*, 34(18):1950137, 2019.
- [39] François Richard. Indications for extra scalars at LHC? – BSM physics at future e^+e^- colliders. 1 2020.
- [40] Stefan Buddenbrock, Alan S. Cornell, Yaquan Fang, Abdualazem Fadol Mohammed, Mukesh Kumar, Bruce Mellado, and Kehinde G. Tomiwa. The emergence of multi-lepton anomalies at the LHC and their compatibility with new physics at the EW scale. *JHEP*, 10:157, 2019.
- [41] T. Robens. Extended scalar sectors at current and future colliders. In *55th Rencontres de Moriond on QCD and High Energy Interactions*, 5 2021.
- [42] Brian Shuve and Itay Yavin. Baryogenesis through Neutrino Oscillations: A Unified Perspective. *Phys. Rev. D*, 89(7):075014, 2014.
- [43] Manfred Lindner and Markus Michael Muller. Comparison of Boltzmann kinetics with quantum dynamics for a chiral Yukawa model far from equilibrium. *Phys. Rev. D*, 77:025027, 2008.
- [44] A. Anisimov, W. Buchmüller, M. Drewes, and S. Mendizabal. Quantum Leptogenesis I. *Annals Phys.*, 326:1998–2038, 2011. [Erratum: *Annals Phys.* 338, 376–377 (2011)].
- [45] Marco Drewes and Jin U Kang. Sterile neutrino Dark Matter production from scalar decay in a thermal bath. *JHEP*, 05:051, 2016.
- [46] Asmaa Abada, Giorgio Arcadi, Valerie Domcke, Marco Drewes, Juraj Klarić, and Michele Lucente. Low-scale leptogenesis with three heavy neutrinos. *JHEP*, 01:164, 2019.
- [47] Michael Dine, Robert G. Leigh, Patrick Huet, Andrei D. Linde, and Dmitri A. Linde. Comments on the electroweak phase transition. *Phys. Lett. B*, 283:319–325, 1992.